Thermochimica Acta, 162 (1990) 435–444
Elsevier Science Publishers B.V., Amsterdam – Printed in The Netherlands

THERMAL DECOMPOSITION AND REDUCTION WITH H_2 AND C_2H_4 OF SILVER(I,II) OXIDE

P. TISSOT, H. LARTIGUE and J.F. ROSSIGNOL

Département de Chimie Minérale, Analytique et Appliquée, Université de Genève, 30 quai E. Ansermet, 1211 Genève 4 (Switzerland)

(Received 14 November 1989)

ABSTRACT

Two types of AgO (monoclinic and tetragonal) have been studied by thermogravimetry. The thermal decomposition of AgO to AgO_2 proceeds according to a nucleation-growth mechanism, A_2. The introduction of nuclei of Ag_2O modifies the mechanism to a propagation law, R_3, but only when the nuclei are made by thermal decomposition.

The reduction of AgO with hydrogen gives silver in one step, but with ethylene the reduction proceeds in two steps, with the intermediate formation of Ag_2O.

INTRODUCTION

The thermal behaviour and the reduction with H_2 and C_2H_4 of two types of silver oxide have been studied: one is monoclinic [1], hereafter referred to as OSK, and the other is tetragonal [2,3], referred to as OS.

This study is based essentially on the interpretation of isothermal thermogravimetric curves in order to determine the most probable mechanism of the reaction and the apparent kinetic parameters according to the Arrhenius equation [4]. The criterion for selection of the mechanism is the best fit with a model; in every case a correlation factor better than 0.999 is required for a linear fit.

EXPERIMENTAL

The syntheses of the silver oxides OSK and OS have already been described [1,2]. Monocrystals of monoclinic AgO have also been prepared by the electrochemical method described by Jansen and Fischer [5] to try to confirm the mechanism by microscopic examination during the reaction. For this purpose, we have developed an air-tight heating stage; the temperature of the sample can be controlled between 25 and 300 °C, within 0.1 °C. The

0040-6031/90/$03.50

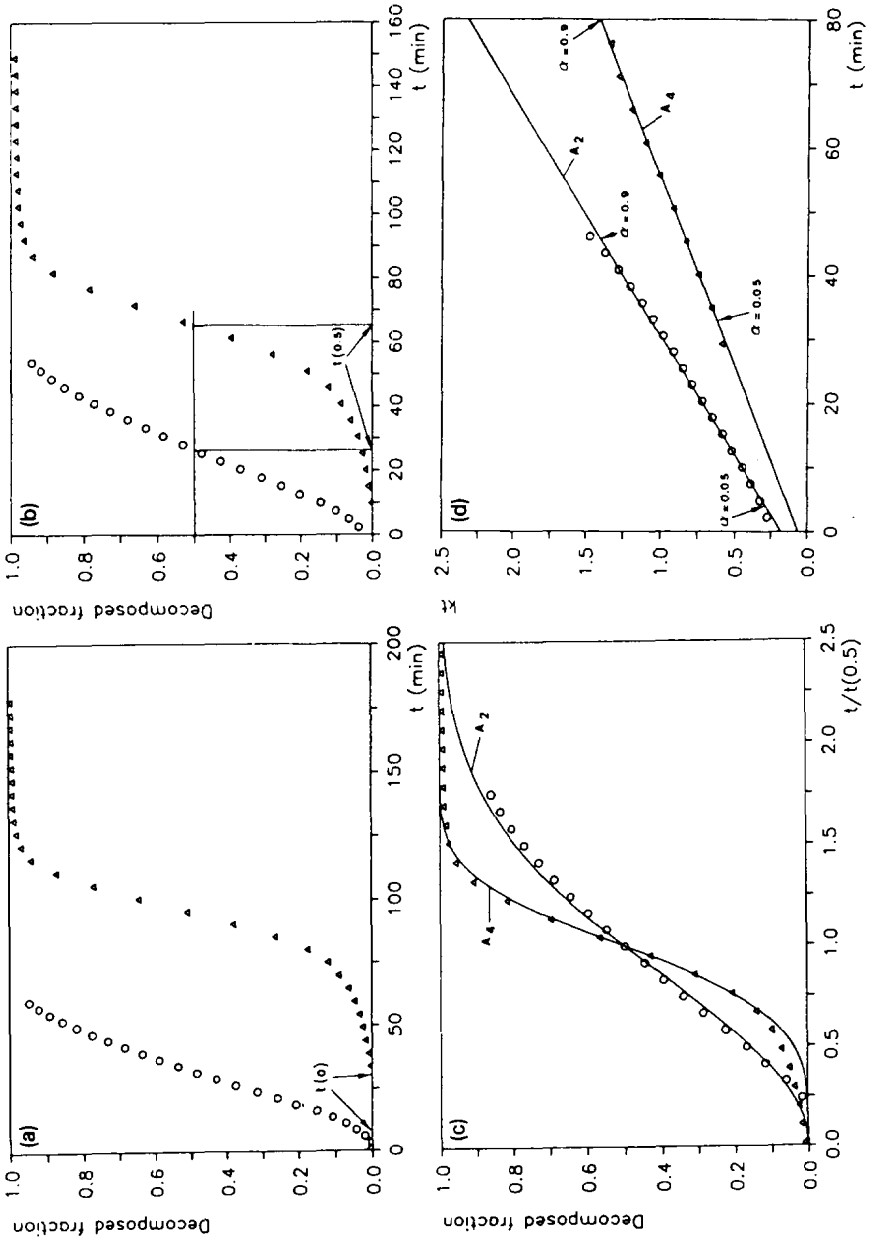

Fig. 1. Reduction of AgO to Ag with H_2: ▲, OSK; ○, OS; temp., 67 °C. a, Experimental curves, $t(0) = 30$ min for OSK and 8 min for OS. b, Corrected curves, $t(0.5) = 65$ min for OSK and 27 min for OS. c, Reduced curves: A_2, $\alpha = 1 - e[-(0.8326\ t/t(0.5))^2]$ and A_4, $\alpha = 1 - e[-0.9214\ t/t(0.5))^4]$. d, Linear fitting: A_2, $kt = [-\ln(1-\alpha)]^{1/2}$ and A_4, $kt = [-\ln(1-\alpha)]^{1/4}$.

evolution of the sample is followed by video recording, with a magnification of 400 ×.

A commercial sample of monoclinic AgO, obtained by oxidation of silver ions with persulphate, was also tested for comparison in the case of the thermal decomposition. The composition of the silver oxides used in this work were: OSK, ≈ 96% AgO, ≈ 4% Ag_2O and traces of Ag_2CO_3; OS, ≈ 99% AgO and traces of Ag_2CO_3; monocrystals, ≈ 99% AgO; and commercial, ≈ 95% AgO, ≈ 5% Ag_2O and traces of Ag_2CO_3.

To minimise the non-steady-state period between the introduction of the sample in the furnace of the thermobalance and the moment when constant temperature is reached, we have adapted a balance (Setaram B70) with a device especially designed to optimise the heat transfer, so that measurement of the curve can begin after 5 min. The weight of the sample (~ 45 mg) is memorised every 30 s with a data acquisition device (Wavetek 52) and processed by means of a program developed in our laboratory.

Figure 1 represents an example of two isothermal thermogravimetric curves processed to determine the most probable mechanism of the reaction: Fig. 1a shows the experimental curves. From the weight loss measured at the end of the experiment, $t(0)$, corresponding to the beginning of the reaction can be determined. This induction period varies from 5 min to more than 1 h depending on the nature of the sample and the experimental conditions; here it was 8 and 30 min. The corrected curves are shown in Fig. 1b with the measurement of $t(0.5)$, corresponding to $\alpha = 0.5$. Figures 1c and 1d show the determination of the mechanism by comparison of the reduced curve with a model [5] (Fig. 1c) and by the linear fit of the equation corresponding to the chosen mechanism (Fig. 1d). The slope of these straight lines is the rate constant, from which the apparent activation energy and the pre-exponential factor of the Arrhenius equation can be determined.

The labels used for the different mechanisms are those given by Sharp et al. [6].

RESULTS AND DISCUSSION

Thermal decomposition of AgO to Ag_2O

AgO is not thermodynamically stable at room temperature and starts to decompose perceptibly to Ag_2O at around 100 °C, according to the equation

$$2AgO = Ag_2O + 0.5O_2 \quad (1)$$

Table 1 and Fig. 2 show the results obtained for four samples. In all cases the decomposition follows the same mechanism for all the temperatures studied: A_2 for $0.05 \leqslant \alpha \leqslant 0.6$ and R_3 for $0.7 \leqslant \alpha \leqslant 0.95$. On the other hand, the induction time and the kinetic factors depend on the morphology

TABLE 1

Thermal decomposition of AgO in nitrogen

Sample	Mecha-nism	α range	$t(0)$ (min)	Temp. range (°C)	E_a (kJ mol^{-1})	ln k_0
OSK	A_2	0.05–0.6	5– 7	125–170	110	28
Commercid	A_2	0.05–0.6	5– 7	125–170	110	28
OS	A_2	0.05–0.6	5– 7	125–150	122	32
Crystals	A_2	0.05–0.6	20–30	125–170	140	36

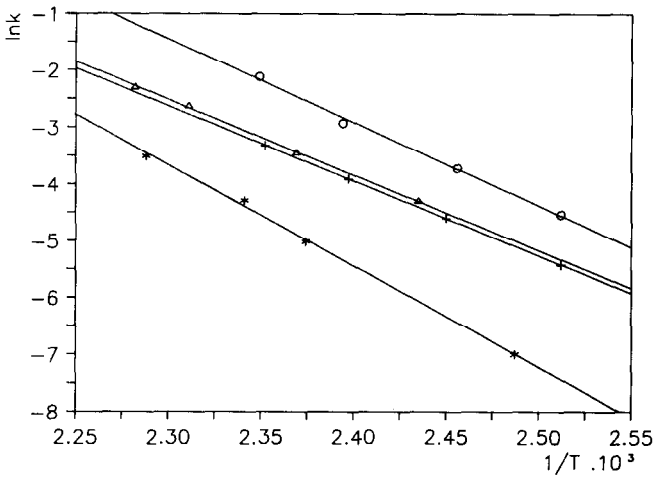

Fig. 2. Arrhenius plots for the thermal decomposition of AgO to Ag_2O in nitrogen: ○, OS; △, OSK; +, commercial sample; and *, monocrystals.

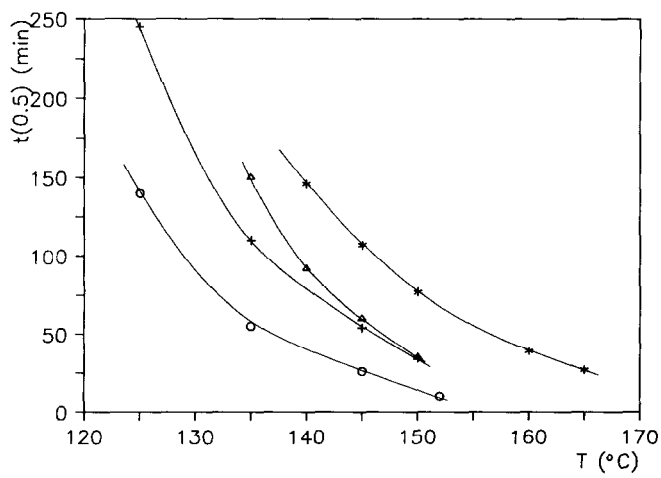

Fig. 3. $t(0.5)$ as a function of temperature for the thermal decomposition of AgO in nitrogen: ○, OS; △, OSK; +, commercial sample, and *, monocrystals.

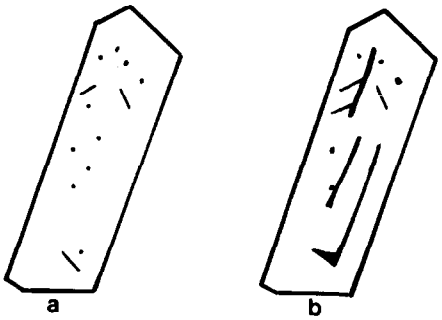

Fig. 4. Microscopic evolution of the thermal decomposition of a monocrystal of AgO in nitrogen at 140 °C (magnification, 200×): a, after 10 min; b, after 30 min.

and/or the allotropic form of the samples. The rate of the reaction is also very different, as shown in Fig. 3. The tetragonal form is less stable than the monoclinic. The particle size also influences the decomposition rate, as can be seen in the differences between the commercial sample (0.1–1 μm), the OSK (10–30 μm) and the crystals (100–300 μm). The microscopic observation of a monocrystal in reflected light at 140 °C in nitrogen (Fig. 4) seems to confirm the nucleation-growth process in two dimensions (A_2).

Thermal decomposition of a mixture of AgO and AgO_2

To a sample of OSK was added ≈ 25% of Ag_2O prepared in three different ways. One sample was partially reduced with H_2 at 30 °C

$$AgO \xrightarrow[-H_2O]{H_2} AgO + Ag_2O \qquad (OSKH_2) \tag{2}$$

Another was partially decomposed in nitrogen at 125 °C

$$AgO \xrightarrow[-O_2]{\Delta} AgO + Ag_2O \qquad (OSK\Delta) \tag{3}$$

The third was prepared by interrupting the oxidation of Ag before the end of the synthesis reaction

$$Ag \xrightarrow[-O_2]{O_3} AgO + Ag_2O \qquad (OSKO_3) \tag{4}$$

The mechanism of the thermal decomposition of these samples has been determined at 130 and 160 °C in nitrogen and the results are indicated in Table 2. It is interesting to note that AgOΔ is the only sample which shows a modified mechanism; only in that case does the formation of Ag_2O correspond to the nucleation step of the thermal decomposition, so that a propagation law is observed from $\alpha = 0.05$, see Fig. 5. The decomposed fraction is represented here as $\alpha = 1$ for the total decomposition of a sample containing ≈ 75% AgO. Observation by scanning electron microscopy of the samples which were partially reduced with H_2 ($OSKH_2$) and of those

TABLE 2

Thermal decomposition of $AgO + Ag_2O$ in nitrogen at 130 and 160 °C

Sample	Mechanism	σ range
$OSKH_2$	A_2	0.05–0.6
	R_2-R_3	0.7 –0.9
OSKΔ	R_2-R_3	0.05–0.9
$OSKO_3$	A_2	0.05–0.6
	R_2-R_3	0.7 –0.9

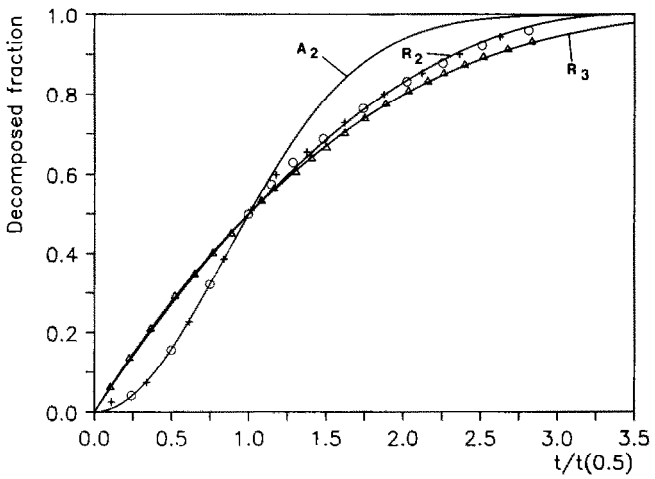

Fig. 5. Reduced plots for the thermal decomposition of AgO containing ≈ 25% of Ag_2O at 165 °C in nitrogen: +, $OSKH_2$; ○, $OSKO_3$; and △, OSKΔ. A_2, $\alpha = 1 - e[-(0.8326\, t/t(0.5))^2]$; R_2, $\alpha = 1 - (1 - 0.2929\, t/t(0.5))^2$; and R_3, $\alpha = 1 - (1 - 0.2063\, t/t(0.5))^3$.

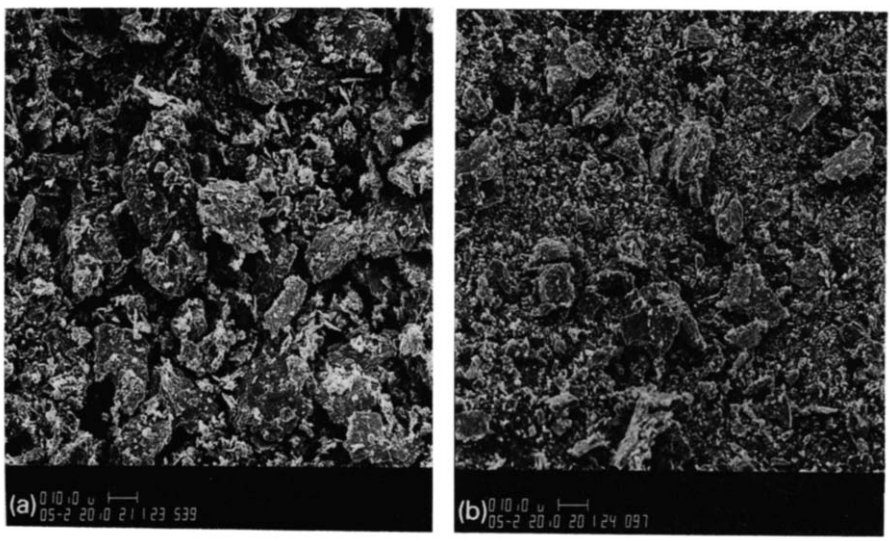

Fig. 6. Scanning electron microscopy of partially reduced AgO (≈ 75% AgO– ≈ 25% Ag_2O): a, $OSKH_2$; b, OSKΔ.

partially decomposed (OSHΔ) (Fig. 6) shows that only the latter preserves the original morphology of the OSK type of AgO [1]; the nuclei of Ag_2O have grown on the surface of the AgO and are still in contact with it; this is not the case for the $OSKH_2$ which has broken into small particles.

Reduction of AgO with H_2

Both types of AgO (OSK and OS) are reduced by hydrogen to silver in one step with the intermediate formation of Ag_2O, according to

$$2AgO + H_2 = Ag_2O + H_2O \quad (5)$$

and

$$Ag_2O + H_2 = 2Ag + H_2O \quad (6)$$

as indicated by the analysis of partially reduced samples, see Table 3. The analysis was performed by thermogravimetry, as described in ref. 1.

Figure 7 shows, however, that only one mechanism is followed during the reduction; this probably means that the first reaction (eqn. (5)) is the rate-determining step, and that the mechanism and the kinetic parameters correspond to the formation of Ag_2O. The behaviour of this oxide formed by the reduction of AgO is different from that of pure Ag_2O, and its reducibility by hydrogen is much higher, perhaps due to a catalytic action of AgO or to a reactive form of Ag_2O. The reduction of Ag_2O to Ag with H_2 has been studied by Nakamori et al. [7] who have determined an apparent activation energy of 104 kJ mol^{-1} for this reaction, a value much higher than that obtained here for the reduction of AgO; to agree with our hypothesis that the rate-determining step is the reduction of AgO to Ag_2O, the reverse should apply.

TABLE 3

Analysis of AgO partially reduced with H_2

Sample	Reduction temp. [°C]	Point [a]	α	AgO (%)	Ag_2O (%)	Ag (%)
OSK	43	1	0.47	30	46	24
OS	43	2	0.48	10	82	8
OSK	67	3	0.20	56	44	0
OSK	67	4	0.35	35	60	5
OSK	67	5	0.49	18	66	16
OSK	67	6	0.74	12	28	60
OS	67	7	0.18	67	33	0
OS	67	8	0.32	45	55	0
OS	67	9	0.46	27	58	15

[a] See Fig. 7.

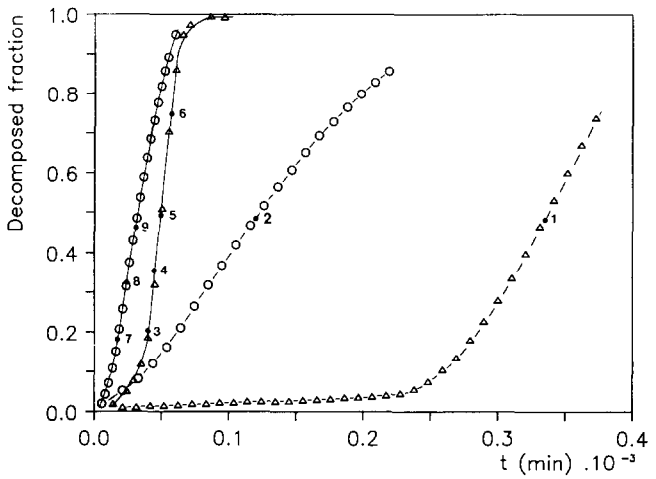

Fig. 7. Corrected curves for the reduction of AgO with H_2: —△—, OSK, 43°C; △——△, OSK, 67°C; —○—, OS, 43°C; and ○——○, OS, 67°C.

TABLE 4

Reduction of AgO to Ag with hydrogen

Sample	Mechanism	α range	$t(0)$ (min)	Temp. range (°C)	E_a (kJ mol^{-1})	ln k_0
OSK	A_4	0.05–0.9	30–60	43–67	55	15.8
OS	A_2	0.05–0.9	6–20	43–67	56	16.2

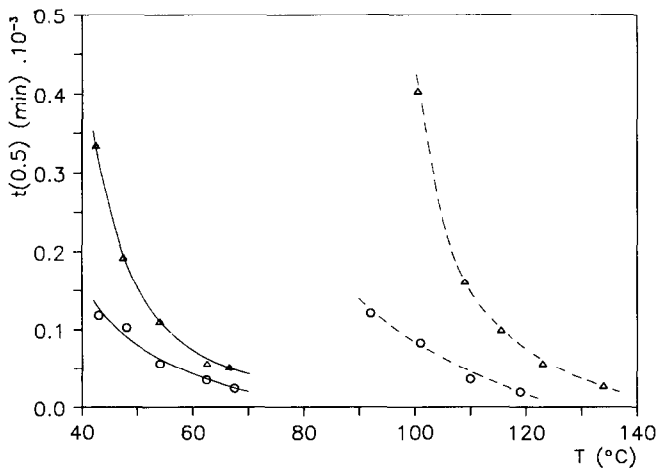

Fig. 8. $t(0.5)$ as a function of temperature for the reduction of AgO with H_2 and C_2H_4: —○—, OS in H_2; ○——○, OS in C_2H_4; —△—, OSK in H_2; and △——△, OSK in C_2H_4.

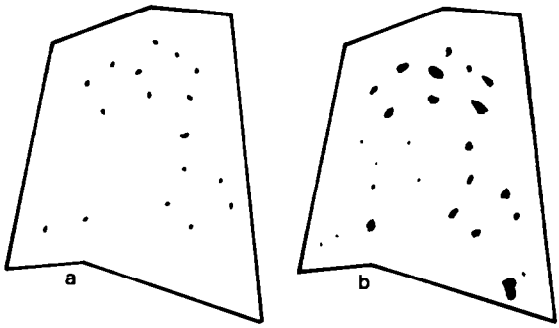

Fig. 9. Microscopic evolution of the reduction of a monocrystal of AgO in H_2 (heating rate 1°C min^{-1}): a, 90°C; b, 120°C.

However, in spite of the complexity of the reduction of AgO to Ag by hydrogen, an A_4 mechanism for OSK and A2 for OS are very closely followed at all the temperatures tested; the results are indicated in Table 4.

The induction period, $t(0)$, is much longer for the monoclinic form (OSK) than for the tetragonal one (OS). The rate of the reduction (Fig. 8) is higher for OS than for OSK, as is the case for the thermal decomposition (Fig. 3). Figure 9 shows the course of the reduction of a monoclinic crystal observed with a magnification of 400 ×; this is different from the thermal decomposition (Fig. 4) and seems to be in agreement with a three-dimensional growth of the nucleus.

Reduction of AgO with C_2H_4

Both types of AgO (OSK and OS) are reduced by ethylene to Ag_2O, and then to Ag in two successive steps, as shown in Fig. 10. The first step (up to $\alpha \approx 0.5$) corresponds to several reactions and is schematically represented by the reaction

$$AgO \xrightarrow{C_2H_4} [Ag_2O, CO_2, H_2O, C_2H_4O] \quad (7)$$

Moreover, the phenomenon is complicated by the partial thermal decomposition of AgO which occurs at the temperature needed for the reaction with C_2H_4 (> 100°C).

Under these conditions, it is not possible to determine the mechanism of the reaction. The analysis of the gas evolved during the reaction in an isothermal reactor [8] shows that the composition of the mixture depends on the nature of the AgO, on the temperature and on the partial pressure of C_2H_4. The second step is represented by

$$Ag_2O \xrightarrow{C_2H_4} [Ag, CO_2, H_2O, C_2H_4O] \quad (8)$$

This reaction proceeds linearly as a function of time, see Fig. 10. As in the

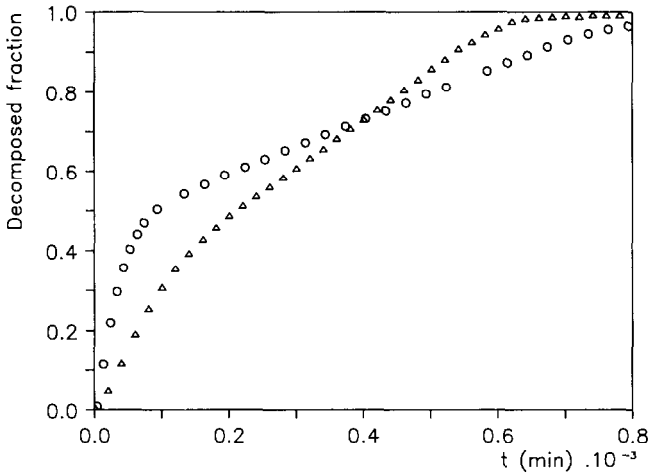

Fig. 10. Decomposed fraction as a function of the time for the reduction of AgO with C_2H_4 ($\alpha = 1$ for the reaction AgO → Ag), at 120 °C: △, OSK; ○, OS.

case of the reduction by hydrogen, this behaviour is different from that observed during the reduction of pure Ag_2O with ethylene, which shows a sigmoïdal curve [7].

A large difference in the velocity of the reduction is observed between OSK and OS: for the first step the reaction is faster for OS, but for the second step, the reaction is faster for OSK (Fig. 8).

ACKNOWLEDGMENT

This work was supported by the Swiss National Foundation for Scientific Research. We thank B. Perrenot for her contribution to a part of this work (Thesis No. 2247, University of Geneva).

REFERENCES

1 R. Dallenbach, J. Painot and P. Tissot, Polyhedron, 1 (1982) 183.
2 P. Tissot, Polyhedron, 6 (1987) 1309.
3 K. Yvon, A. Bezinge, P. Tissot and P. Fischer, J. Solid State Chem., 65 (1986) 225.
4 P. Tissot and B. Perrenot, Thermochim. Acta, 85 (1985) 103.
5 M. Jansen and P. Fischer, J. Less-Common Met., 137 (1988) 123.
6 J.H. Sharp, G.W. Brindley and B.N. Narakar Achar, J. Am. Ceram. Soc., 49 (1966) 379.
7 I. Nakamori, H. Nakamura, T. Hayano and S. Kagawa, Bull. Chem. Soc. Jpn., 47 (1974) 1827.
8 P. Tissot, unpublished results.